Study of D_{sJ} decays to D^*K in inclusive e^+e^- interactions

B. Aubert,[1] Y. Karyotakis,[1] J. P. Lees,[1] V. Poireau,[1] E. Prencipe,[1] X. Prudent,[1] V. Tisserand,[1] J. Garra Tico,[2] E. Grauges,[2] M. Martinelli,[3a,3b] A. Palano,[3a,3b] M. Pappagallo,[3a,3b] G. Eigen,[4] B. Stugu,[4] L. Sun,[4] M. Battaglia,[5] D. N. Brown,[5] B. Hooberman,[5] L. T. Kerth,[5] Yu. G. Kolomensky,[5] G. Lynch,[5] I. L. Osipenkov,[5] K. Tackmann,[5] T. Tanabe,[5] C. M. Hawkes,[6] N. Soni,[6] A. T. Watson,[6] H. Koch,[7] T. Schroeder,[7] D. J. Asgeirsson,[8] C. Hearty,[8] T. S. Mattison,[8] J. A. McKenna,[8] M. Barrett,[9] A. Khan,[9] A. Randle-Conde,[9] V. E. Blinov,[10] A. D. Bukin,[10,*] A. R. Buzykaev,[10] V. P. Druzhinin,[10] V. B. Golubev,[10] A. P. Onuchin,[10] S. I. Serednyakov,[10] Yu. I. Skovpen,[10] E. P. Solodov,[10] K. Yu. Todyshev,[10] M. Bondioli,[11] S. Curry,[11] I. Eschrich,[11] D. Kirkby,[11] A. J. Lankford,[11] P. Lund,[11] M. Mandelkern,[11] E. C. Martin,[11] D. P. Stoker,[11] H. Atmacan,[12] J. W. Gary,[12] F. Liu,[12] O. Long,[12] G. M. Vitug,[12] Z. Yasin,[12] V. Sharma,[13] C. Campagnari,[14] T. M. Hong,[14] D. Kovalskyi,[14] M. A. Mazur,[14] J. D. Richman,[14] T. W. Beck,[15] A. M. Eisner,[15] C. A. Heusch,[15] J. Kroseberg,[15] W. S. Lockman,[15] A. J. Martinez,[15] T. Schalk,[15] B. A. Schumm,[15] A. Seiden,[15] L. Wang,[15] L. O. Winstrom,[15] C. H. Cheng,[16] D. A. Doll,[16] B. Echenard,[16] F. Fang,[16] D. G. Hitlin,[16] I. Narsky,[16] P. Ongmongkolkul,[16] T. Piatenko,[16] F. C. Porter,[16] R. Andreassen,[17] G. Mancinelli,[17] B. T. Meadows,[17] K. Mishra,[17] M. D. Sokoloff,[17] P. C. Bloom,[18] W. T. Ford,[18] A. Gaz,[18] J. F. Hirschauer,[18] M. Nagel,[18] U. Nauenberg,[18] J. G. Smith,[18] S. R. Wagner,[18] R. Ayad,[19,†] W. H. Toki,[19] R. J. Wilson,[19] E. Feltresi,[20] A. Hauke,[20] H. Jasper,[20] T. M. Karbach,[20] J. Merkel,[20] A. Petzold,[20] B. Spaan,[20] K. Wacker,[20] M. J. Kobel,[21] R. Nogowski,[21] K. R. Schubert,[21] R. Schwierz,[21] D. Bernard,[22] E. Latour,[22] M. Verderi,[22] P. J. Clark,[23] S. Playfer,[23] J. E. Watson,[23] M. Andreotti,[24a,24b] D. Bettoni,[24a] C. Bozzi,[24a] R. Calabrese,[24a,24b] A. Cecchi,[24a,24b] G. Cibinetto,[24a,24b] E. Fioravanti,[24a,24b] P. Franchini,[24a,24b] E. Luppi,[24a,24b] M. Munerato,[24a,24b] M. Negrini,[24a,24b] A. Petrella,[24a,24b] L. Piemontese,[24a] V. Santoro,[24a,24b] R. Baldini-Ferroli,[25] A. Calcaterra,[25] R. de Sangro,[25] G. Finocchiaro,[25] S. Pacetti,[25] P. Patteri,[25] I. M. Peruzzi,[25,‡] M. Piccolo,[25] M. Rama,[25] A. Zallo,[25] R. Contri,[26a,26b] E. Guido,[26a] M. Lo Vetere,[26a,26b] M. R. Monge,[26a,26b] S. Passaggio,[26a] C. Patrignani,[26a,26b] E. Robutti,[26a] S. Tosi,[26a,26b] K. S. Chaisanguanthum,[27] M. Morii,[27] A. Adametz,[28] J. Marks,[28] S. Schenk,[28] U. Uwer,[28] F. U. Bernlochner,[29] V. Klose,[29] H. M. Lacker,[29] T. Lueck,[29] A. Volk,[29] D. J. Bard,[30] P. D. Dauncey,[30] M. Tibbetts,[30] P. K. Behera,[31] M. J. Charles,[31] U. Mallik,[31] J. Cochran,[32] H. B. Crawley,[32] L. Dong,[32] V. Eyges,[32] W. T. Meyer,[32] S. Prell,[32] E. I. Rosenberg,[32] A. E. Rubin,[32] Y. Y. Gao,[33] A. V. Gritsan,[33] Z. J. Guo,[33] N. Arnaud,[34] J. Béquilleux,[34] A. D'Orazio,[34] M. Davier,[34] D. Derkach,[34] J. Firmino da Costa,[34] G. Grosdidier,[34] F. Le Diberder,[34] V. Lepeltier,[34] A. M. Lutz,[34] B. Malaescu,[34] S. Pruvot,[34] P. Roudeau,[34] M. H. Schune,[34] J. Serrano,[34] V. Sordini,[34,§] A. Stocchi,[34] G. Wormser,[34] D. J. Lange,[35] D. M. Wright,[35] I. Bingham,[36] J. P. Burke,[36] C. A. Chavez,[36] J. R. Fry,[36] E. Gabathuler,[36] R. Gamet,[36] D. E. Hutchcroft,[36] D. J. Payne,[36] C. Touramanis,[36] A. J. Bevan,[37] C. K. Clarke,[37] F. Di Lodovico,[37] R. Sacco,[37] M. Sigamani,[37] G. Cowan,[38] S. Paramesvaran,[38] A. C. Wren,[38] D. N. Brown,[39] C. L. Davis,[39] A. G. Denig,[40] M. Fritsch,[40] W. Gradl,[40] A. Hafner,[40] K. E. Alwyn,[41] D. Bailey,[41] R. J. Barlow,[41] G. Jackson,[41] G. D. Lafferty,[41] T. J. West,[41] J. I. Yi,[41] J. Anderson,[42] C. Chen,[42] A. Jawahery,[42] D. A. Roberts,[42] G. Simi,[42] J. M. Tuggle,[42] C. Dallapiccola,[43] E. Salvati,[43] R. Cowan,[44] D. Dujmic,[44] P. H. Fisher,[44] S. W. Henderson,[44] G. Sciolla,[44] M. Spitznagel,[44] R. K. Yamamoto,[44] M. Zhao,[44] P. M. Patel,[45] S. H. Robertson,[45] M. Schram,[45] P. Biassoni,[46a,46b] A. Lazzaro,[46a,46b] V. Lombardo,[46a] F. Palombo,[46a,46b] S. Stracka,[46a,46b] L. Cremaldi,[47] R. Godang,[47,‖] R. Kroeger,[47] P. Sonnek,[47] D. J. Summers,[47] H. W. Zhao,[47] M. Simard,[48] P. Taras,[48] H. Nicholson,[49] G. De Nardo,[50a,50b] L. Lista,[50a] D. Monorchio,[50a,50b] G. Onorato,[50a,50b] C. Sciacca,[50a,50b] G. Raven,[51] H. L. Snoek,[51] C. P. Jessop,[52] K. J. Knoepfel,[52] J. M. LoSecco,[52] W. F. Wang,[52] L. A. Corwin,[53] K. Honscheid,[53] H. Kagan,[53] R. Kass,[53] J. P. Morris,[53] A. M. Rahimi,[53] S. J. Sekula,[53] Q. K. Wong,[53] N. L. Blount,[54] J. Brau,[54] R. Frey,[54] O. Igonkina,[54] J. A. Kolb,[54] M. Lu,[54] R. Rahmat,[54] N. B. Sinev,[54] D. Strom,[54] J. Strube,[54] E. Torrence,[54] G. Castelli,[55a,55b] N. Gagliardi,[55a,55b] M. Margoni,[55a,55b] M. Morandin,[55a] M. Posocco,[55a] M. Rotondo,[55a] F. Simonetto,[55a,55b] R. Stroili,[55a,55b] C. Voci,[55a,55b] P. del Amo Sanchez,[56] E. Ben-Haim,[56] G. R. Bonneaud,[56] H. Briand,[56] J. Chauveau,[56] O. Hamon,[56] Ph. Leruste,[56] G. Marchiori,[56] J. Ocariz,[56] A. Perez,[56] J. Prendki,[56] S. Sitt,[56] L. Gladney,[57] M. Biasini,[58a,58b] E. Manoni,[58a,58b] C. Angelini,[59a,59b] G. Batignani,[59a,59b] S. Bettarini,[59a,59b] G. Calderini,[59a,59b,¶] M. Carpinelli,[59a,59b,**] A. Cervelli,[59a,59b] F. Forti,[59a,59b] M. A. Giorgi,[59a,59b] A. Lusiani,[59a,59c] M. Morganti,[59a,59b] N. Neri,[59a,59b] E. Paoloni,[59a,59b] G. Rizzo,[59a,59b] J. J. Walsh,[59a] D. Lopes Pegna,[60] C. Lu,[60] J. Olsen,[60] A. J. S. Smith,[60] A. V. Telnov,[60] F. Anulli,[61a] E. Baracchini,[61a,61b] G. Cavoto,[61a] R. Faccini,[61a,61b] F. Ferrarotto,[61a] F. Ferroni,[61a,61b] M. Gaspero,[61a,61b] P. D. Jackson,[61a] L. Li Gioi,[61a] M. A. Mazzoni,[61a] S. Morganti,[61a] G. Piredda,[61a] F. Renga,[61a,61b] C. Voena,[61a] M. Ebert,[62] T. Hartmann,[62] H. Schröder,[62] R. Waldi,[62] T. Adye,[63] B. Franek,[63] E. O. Olaiya,[63] F. F. Wilson,[63] S. Emery,[64] L. Esteve,[64] G. Hamel de Monchenault,[64] W. Kozanecki,[64] G. Vasseur,[64] Ch. Yèche,[64] M. Zito,[64] M. T. Allen,[65] D. Aston,[65] R. Bartoldus,[65] J. F. Benitez,[65] R. Cenci,[65] J. P. Coleman,[65]

M. R. Convery,[65] J. C. Dingfelder,[65] J. Dorfan,[65] G. P. Dubois-Felsmann,[65] W. Dunwoodie,[65] R. C. Field,[65] M. Franco Sevilla,[65] B. G. Fulsom,[65] A. M. Gabareen,[65] M. T. Graham,[65] P. Grenier,[65] C. Hast,[65] W. R. Innes,[65] J. Kaminski,[65] M. H. Kelsey,[65] H. Kim,[65] P. Kim,[65] M. L. Kocian,[65] D. W. G. S. Leith,[65] S. Li,[65] B. Lindquist,[65] S. Luitz,[65] V. Luth,[65] H. L. Lynch,[65] D. B. MacFarlane,[65] H. Marsiske,[65] R. Messner,[65,*] D. R. Muller,[65] H. Neal,[65] S. Nelson,[65] C. P. O'Grady,[65] I. Ofte,[65] M. Perl,[65] B. N. Ratcliff,[65] A. Roodman,[65] A. A. Salnikov,[65] R. H. Schindler,[65] J. Schwiening,[65] A. Snyder,[65] D. Su,[65] M. K. Sullivan,[65] K. Suzuki,[65] S. K. Swain,[65] J. M. Thompson,[65] J. Va'vra,[65] A. P. Wagner,[65] M. Weaver,[65] C. A. West,[65] W. J. Wisniewski,[65] M. Wittgen,[65] D. H. Wright,[65] H. W. Wulsin,[65] A. K. Yarritu,[65] C. C. Young,[65] V. Ziegler,[65] X. R. Chen,[66] H. Liu,[66] W. Park,[66] M. V. Purohit,[66] R. M. White,[66] J. R. Wilson,[66] M. Bellis,[67] P. R. Burchat,[67] A. J. Edwards,[67] T. S. Miyashita,[67] S. Ahmed,[68] M. S. Alam,[68] J. A. Ernst,[68] B. Pan,[68] M. A. Saeed,[68] S. B. Zain,[68] A. Soffer,[69] S. M. Spanier,[70] B. J. Wogsland,[70] R. Eckmann,[71] J. L. Ritchie,[71] A. M. Ruland,[71] C. J. Schilling,[71] R. F. Schwitters,[71] B. C. Wray,[71] B. W. Drummond,[72] J. M. Izen,[72] X. C. Lou,[72] F. Bianchi,[73a,73b] D. Gamba,[73a,73b] M. Pelliccioni,[73a,73b] M. Bomben,[74a,74b] L. Bosisio,[74a,74b] C. Cartaro,[74a,74b] G. Della Ricca,[74a,74b] L. Lanceri,[74a,74b] L. Vitale,[74a,74b] V. Azzolini,[75] N. Lopez-March,[75] F. Martinez-Vidal,[75] D. A. Milanes,[75] A. Oyanguren,[75] J. Albert,[76] Sw. Banerjee,[76] B. Bhuyan,[76] H. H. F. Choi,[76] K. Hamano,[76] G. J. King,[76] R. Kowalewski,[76] M. J. Lewczuk,[76] I. M. Nugent,[76] J. M. Roney,[76] R. J. Sobie,[76] T. J. Gershon,[77] P. F. Harrison,[77] J. Ilic,[77] T. E. Latham,[77] G. B. Mohanty,[77] E. M. T. Puccio,[77] H. R. Band,[78] X. Chen,[78] S. Dasu,[78] K. T. Flood,[78] Y. Pan,[78] R. Prepost,[78] C. O. Vuosalo,[78] and S. L. Wu[78]

(*BABAR* Collaboration)

[1]*Laboratoire d'Annecy-le-Vieux de Physique des Particules (LAPP), Université de Savoie, CNRS/IN2P3, F-74941 Annecy-Le-Vieux, France*
[2]*Universitat de Barcelona, Facultat de Fisica, Departament ECM, E-08028 Barcelona, Spain*
[3a]*INFN Sezione di Bari, I-70126 Bari, Italy*
[3b]*Dipartimento di Fisica, Università di Bari, I-70126 Bari, Italy*
[4]*University of Bergen, Institute of Physics, N-5007 Bergen, Norway*
[5]*Lawrence Berkeley National Laboratory and University of California, Berkeley, California 94720, USA*
[6]*University of Birmingham, Birmingham, B15 2TT, United Kingdom*
[7]*Ruhr Universität Bochum, Institut für Experimentalphysik 1, D-44780 Bochum, Germany*
[8]*University of British Columbia, Vancouver, British Columbia, Canada V6T 1Z1*
[9]*Brunel University, Uxbridge, Middlesex UB8 3PH, United Kingdom*
[10]*Budker Institute of Nuclear Physics, Novosibirsk 630090, Russia*
[11]*University of California at Irvine, Irvine, California 92697, USA*
[12]*University of California at Riverside, Riverside, California 92521, USA*
[13]*University of California at San Diego, La Jolla, California 92093, USA*
[14]*University of California at Santa Barbara, Santa Barbara, California 93106, USA*
[15]*University of California at Santa Cruz, Institute for Particle Physics, Santa Cruz, California 95064, USA*
[16]*California Institute of Technology, Pasadena, California 91125, USA*
[17]*University of Cincinnati, Cincinnati, Ohio 45221, USA*
[18]*University of Colorado, Boulder, Colorado 80309, USA*
[19]*Colorado State University, Fort Collins, Colorado 80523, USA*
[20]*Technische Universität Dortmund, Fakultät Physik, D-44221 Dortmund, Germany*
[21]*Technische Universität Dresden, Institut für Kern- und Teilchenphysik, D-01062 Dresden, Germany*
[22]*Laboratoire Leprince-Ringuet, CNRS/IN2P3, Ecole Polytechnique, F-91128 Palaiseau, France*
[23]*University of Edinburgh, Edinburgh EH9 3JZ, United Kingdom*
[24a]*INFN Sezione di Ferrara, I-44100 Ferrara, Italy*
[24b]*Dipartimento di Fisica, Università di Ferrara, I-44100 Ferrara, Italy*
[25]*INFN Laboratori Nazionali di Frascati, I-00044 Frascati, Italy*
[26a]*INFN Sezione di Genova, I-16146 Genova, Italy*
[26b]*Dipartimento di Fisica, Università di Genova, I-16146 Genova, Italy*
[27]*Harvard University, Cambridge, Massachusetts 02138, USA*
[28]*Universität Heidelberg, Physikalisches Institut, Philosophenweg 12, D-69120 Heidelberg, Germany*
[29]*Humboldt-Universität zu Berlin, Institut für Physik, Newtonstrasse 15, D-12489 Berlin, Germany*
[30]*Imperial College London, London, SW7 2AZ, United Kingdom*
[31]*University of Iowa, Iowa City, Iowa 52242, USA*
[32]*Iowa State University, Ames, Iowa 50011-3160, USA*
[33]*Johns Hopkins University, Baltimore, Maryland 21218, USA*

[34]*Laboratoire de l'Accélérateur Linéaire, IN2P3/CNRS et Université Paris-Sud 11, Centre Scientifique d'Orsay, B. P. 34, F-91898 Orsay Cedex, France*
[35]*Lawrence Livermore National Laboratory, Livermore, California 94550, USA*
[36]*University of Liverpool, Liverpool L69 7ZE, United Kingdom*
[37]*Queen Mary, University of London, London, E1 4NS, United Kingdom*
[38]*University of London, Royal Holloway and Bedford New College, Egham, Surrey TW20 0EX, United Kingdom*
[39]*University of Louisville, Louisville, Kentucky 40292, USA*
[40]*Johannes Gutenberg-Universität Mainz, Institut für Kernphysik, D-55099 Mainz, Germany*
[41]*University of Manchester, Manchester M13 9PL, United Kingdom*
[42]*University of Maryland, College Park, Maryland 20742, USA*
[43]*University of Massachusetts, Amherst, Massachusetts 01003, USA*
[44]*Massachusetts Institute of Technology, Laboratory for Nuclear Science, Cambridge, Massachusetts 02139, USA*
[45]*McGill University, Montréal, Québec, Canada H3A 2T8*
[46a]*INFN Sezione di Milano, I-20133 Milano, Italy*
[46b]*Dipartimento di Fisica, Università di Milano, I-20133 Milano, Italy*
[47]*University of Mississippi, University, Mississippi 38677, USA*
[48]*Université de Montréal, Physique des Particules, Montréal, Québec, Canada H3C 3J7*
[49]*Mount Holyoke College, South Hadley, Massachusetts 01075, USA*
[50a]*INFN Sezione di Napoli, I-80126 Napoli, Italy*
[50b]*Dipartimento di Scienze Fisiche, Università di Napoli Federico II, I-80126 Napoli, Italy*
[51]*NIKHEF, National Institute for Nuclear Physics and High Energy Physics, NL-1009 DB Amsterdam, The Netherlands*
[52]*University of Notre Dame, Notre Dame, Indiana 46556, USA*
[53]*Ohio State University, Columbus, Ohio 43210, USA*
[54]*University of Oregon, Eugene, Oregon 97403, USA*
[55a]*INFN Sezione di Padova, I-35131 Padova, Italy*
[55b]*Dipartimento di Fisica, Università di Padova, I-35131 Padova, Italy*
[56]*Laboratoire de Physique Nucléaire et de Hautes Energies, IN2P3/CNRS, Université Pierre et Marie Curie-Paris6, Université Denis Diderot-Paris7, F-75252 Paris, France*
[57]*University of Pennsylvania, Philadelphia, Pennsylvania 19104, USA*
[58a]*INFN Sezione di Perugia, I-06100 Perugia, Italy*
[58b]*Dipartimento di Fisica, Università di Perugia, I-06100 Perugia, Italy*
[59a]*INFN Sezione di Pisa, I-56127 Pisa, Italy*
[59b]*Dipartimento di Fisica, Università di Pisa, I-56127 Pisa, Italy*
[59c]*Scuola Normale Superiore di Pisa, I-56127 Pisa, Italy*
[60]*Princeton University, Princeton, New Jersey 08544, USA*
[61a]*INFN Sezione di Roma, I-00185 Roma, Italy*
[61b]*Dipartimento di Fisica, Università di Roma La Sapienza, I-00185 Roma, Italy*
[62]*Universität Rostock, D-18051 Rostock, Germany*
[63]*Rutherford Appleton Laboratory, Chilton, Didcot, Oxon, OX11 0QX, United Kingdom*
[64]*CEA, Irfu, SPP, Centre de Saclay, F-91191 Gif-sur-Yvette, France*
[65]*SLAC National Accelerator Laboratory, Stanford, California 94309, USA*
[66]*University of South Carolina, Columbia, South Carolina 29208, USA*
[67]*Stanford University, Stanford, California 94305-4060, USA*
[68]*State University of New York, Albany, New York 12222, USA*
[69]*Tel Aviv University, School of Physics and Astronomy, Tel Aviv, 69978, Israel*
[70]*University of Tennessee, Knoxville, Tennessee 37996, USA*
[71]*University of Texas at Austin, Austin, Texas 78712, USA*
[72]*University of Texas at Dallas, Richardson, Texas 75083, USA*
[73a]*INFN Sezione di Torino, I-10125 Torino, Italy*
[73b]*Dipartimento di Fisica Sperimentale, Università di Torino, I-10125 Torino, Italy*
[74a]*INFN Sezione di Trieste, I-34127 Trieste, Italy*

---

[*]Deceased.
[†]Now at Temple University, Philadelphia, PA 19122, USA.
[‡]Also with Università di Perugia, Dipartimento di Fisica, Perugia, Italy.
[§]Also with Università di Roma La Sapienza, I-00185 Roma, Italy.
[‖]Now at University of South Alabama, Mobile, AL 36688, USA.
[¶]Also with Laboratoire de Physique Nucléaire et de Hautes Energies, IN2P3/CNRS, Université Pierre et Marie Curie-Paris6, Université Denis Diderot-Paris7, F-75252 Paris, France.
[**]Also with Università di Sassari, Sassari, Italy.

[74b]*Dipartimento di Fisica, Università di Trieste, I-34127 Trieste, Italy*
[75]*IFIC, Universitat de Valencia-CSIC, E-46071 Valencia, Spain*
[76]*University of Victoria, Victoria, British Columbia, Canada V8W 3P6*
[77]*Department of Physics, University of Warwick, Coventry CV4 7AL, United Kingdom*
[78]*University of Wisconsin, Madison, Wisconsin 53706, USA*
(Received 6 August 2009; published 9 November 2009)

We observe the decays $D_{s1}^*(2710)^+ \to D^*K$ and $D_{sJ}^*(2860)^+ \to D^*K$ and measure their branching fractions relative to the DK final state. We also observe, in the D^*K mass spectrum, a new broad structure at a mass of $(3044 \pm 8_{\rm stat}(^{+30}_{-5})_{\rm syst})$ MeV$/c^2$ having a width $\Gamma = (239 \pm 35_{\rm stat}(^{+46}_{-42})_{\rm syst})$ MeV. To obtain this result we use 470 fb^{-1} of data recorded by the *BABAR* detector at the PEP-II asymmetric-energy e^+e^- storage rings at the Stanford Linear Accelerator Center running at center-of-mass energies near 10.6 GeV.

DOI: 10.1103/PhysRevD.80.092003 PACS numbers: 14.40.Lb, 13.25.Ft, 12.40.Yx

I. INTRODUCTION

The spectrum of known $c\bar{s}$ states can be described as two S-wave states (D_s^+, D_s^{*+}) with $J^P = 0^-$, 1^-, and four P-wave states $[D_{s0}^*(2317)^+, D_{s1}(2460)^+, D_{s1}(2536)^+, D_{s2}^*(2573)^+]$ with $J^P = 0^+$, 1^+, 1^+, 2^+. Whether this picture is correct remains controversial because the states at 2317 MeV$/c^2$ and 2460 MeV$/c^2$ [1] had been expected to lie at much higher masses [2]. Since the discovery of the new D_s^+ mesons, much theoretical work has been done; however, new experimental results are needed in order to understand this sector of spectroscopy.

Recently, two new D_s^+ mesons have been discovered, $D_{s1}^*(2710)^+$ [3,4] and $D_{sJ}^*(2860)^+$ [3]. The analysis of $D_{s1}^*(2710)^+$ produced in B decays gives the assignment $J^P = 1^-$. For $D_{sJ}^*(2860)^+$, assignments of $J^P = 0^+$ [5,6] and $J^P = 3^-$ [7] have been proposed.

We report here on a search for new D_{sJ}^+ mesons in the mass spectrum of $D^{(*)}K$ inclusively produced at the PEP-II asymmetric-energy e^+e^- storage rings and recorded by the *BABAR* detector. This paper is organized as follows. In Sec. II we give a short description of the *BABAR* experiment, and in Sec. III we describe the data selection. Section IV is devoted to the study of the DK system, and in Sec. V we present the study of the D^*K system. In Sec. VI we describe fits to the D^*K mass spectrum, while in Sec. VII we present an analysis of the angular distributions. Measurements of ratios of branching fractions are described in Sec. VIII, and we summarize the results in Sec. IX.

II. THE *BABAR* EXPERIMENT

This analysis is based on a 470 fb^{-1} data sample recorded at the $\Upsilon(4S)$ resonance and 40 MeV below the resonance. The *BABAR* detector is described in detail elsewhere [8]. We mention here only the parts of the detector which are used in the present analysis. Charged particles are detected and their momenta measured with a combination of a cylindrical drift chamber (DCH) and a silicon vertex tracker (SVT), both operating within the 1.5 T magnetic field of a superconducting solenoid. Information from a ring-imaging Cherenkov detector combined with energy-loss measurements in the SVT and DCH provide identification of charged kaon and pion candidates. The energies and locations of showers associated with photons are measured with a CsI(Tl) electromagnetic calorimeter.

III. DATA SELECTION

We reconstruct the inclusive processes [9] listed in Table I. A particle identification algorithm is applied to all the tracks. Charged kaon identification has an average efficiency of 90% within the acceptance of the detector and an average pion-to-kaon misidentification probability of 1.5% per particle.

For all channels we perform a vertex fit for the D^0 and D^+ daughters and require a χ^2 probability greater than 0.1%. For the π^0 candidates in channels (3), (4), and (6), we combine all photons with energy greater than 30 MeV in pairs, perform a fit with a π^0 mass constraint, and require a χ^2 probability greater than 1%. For the $D^0 \to K^-\pi^+\pi^0$ decay channel we also perform a kinematic fit with a D^0 mass constraint. We obtain $K_S^0 \to \pi^+\pi^-$ candidates by means of a vertex fit and require a χ^2 probability greater than 2%. We accept only K_S^0 candidates with decay length greater than 0.5 cm. To obtain $D^{*+}K_S^0$ candidates, where $D^{*+} \to D^0\pi^+$, we combine fitted D^0 and K_S^0 candidates with a π^+ candidate using a vertex fit which con-

TABLE I. List of reconstructed final states. Here X indicates the rest of the event, with any number of charged or neutral particles.

Channel reaction	D^* decay mode	D decay mode
(1) $e^+e^- \to D^0K^+X$		$D^0 \to K^-\pi^+$
(2) $e^+e^- \to D^+K_S^0X$		$D^+ \to K^-\pi^+\pi^+$
(3) $e^+e^- \to D^{*0}K^+X$	$D^{*0} \to D^0\pi^0$	$D^0 \to K^-\pi^+$
(4) $e^+e^- \to D^{*+}K_S^0X$	$D^{*+} \to D^+\pi^0$	$D^+ \to K^-\pi^+\pi^+$
(5) $e^+e^- \to D^{*+}K_S^0X$	$D^{*+} \to D^0\pi^+$	$D^0 \to K^-\pi^+$
(6) $e^+e^- \to D^{*+}K_S^0X$	$D^{*+} \to D^0\pi^+$	$D^0 \to K^-\pi^+\pi^0$
(7) $e^+e^- \to D^{*+}K_S^0X$	$D^{*+} \to D^0\pi^+$	$D^0 \to K^-\pi^+\pi^+\pi^-$

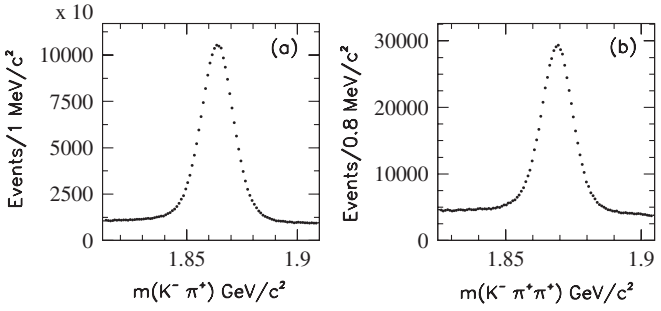

FIG. 1. (a) $K^-\pi^+$ and (b) $K^-\pi^+\pi^+$ mass distributions for all candidate events in channels (1) and (2), respectively.

strains the overall vertex to be located in the interaction region, requiring a χ^2 probability greater than 0.1%. Similarly, for $D^{*+}K_S^0$ candidates where $D^{*+} \to D^+\pi^0$, we combine fitted D^+, K_S^0, and π^0 candidates using a vertex fit which constrains the overall vertex to be located in the interaction region, requiring a χ^2 probability greater than 0.1%. Background from $e^+e^- \to B\bar{B}$ events is removed by requiring the center-of-mass momentum p^* of the DK or D^*K system to be greater than 3.3 GeV/c.

To improve the signal-to-background ratio for channels with $D^0 \to K^-\pi^+$, we study the distribution of the angle θ_{K^-} formed by the K^- from D^0 decay in the $K^-\pi^+$ rest frame with respect to the $K^-\pi^+$ direction in the laboratory system. This distribution is expected to be flat. We observe an accumulation of combinatorial background close to $\cos\theta_{K^-} = 1$. We improve the signal-to-background ratio by requiring $\cos\theta_{K^-} < 0.9$.

To improve the signal-to-background ratio for $D^+ \to K^-\pi^+\pi^+$, we compare the D^+ three-momentum and its flight direction and define d_{xy} as the signed projected distance in the transverse plane. Background events are removed by requiring $d_{xy} > 0$. The resulting $K^-\pi^+$ and $K^-\pi^+\pi^+$ invariant-mass spectra for candidates in channels (1) (where we require in addition a reconstructed K^+) and (2) (where we require in addition a reconstructed K_S^0) are shown in Fig. 1. There are on average 1.01 candidates per selected event in both samples, and all candidates are retained for further analysis.

We fit the $K^-\pi^+$ and $K^-\pi^+\pi^+$ invariant-mass spectra using a linear background and a single-Gaussian peak obtaining $\sigma_{D^0} = 7.6\text{MeV}/c^2$ and $\sigma_{D^+} = 6$ MeV/c^2. The signal region is defined within $\pm 2\sigma$ while sideband regions are defined within $(-6\sigma, -4\sigma)$ and $(4\sigma, 6\sigma)$. The D^0 signal region contains 1.98×10^6 combinations with a purity $P = N_S/(N_S + N_B) = 0.84$, where N_S (N_B) is the number of signal (background) combinations. The D^+ signal region contains 0.58×10^6 combinations with a purity $P = 0.75$.

IV. STUDY OF THE DK SYSTEMS

We first study the D^0K^+ and $D^+K_S^0$ mass spectra. In an inclusive environment the D^0 and D^+ can come from D^* decays. Candidate D^0K^+ pairs where the D^0 is a D^*-decay product are identified by forming $D^0\pi^+$, $D^0\pi^0$, and $D\gamma$ combinations and requiring that the invariant-mass difference between one of those combinations and the D^0 be within $\pm 2\sigma$ of the known $D^* - D$ mass difference. Events belonging to these possible reflections (except for $D^{*0} \to D^0\gamma$ events, which could not be isolated cleanly) are removed. In the same way, $D^+K_S^0$ combinations where the $D^+\pi^0$ and D^+ invariant-mass difference is found to be within $\pm 2\sigma$ of the known $D^* - D$ mass difference are removed.

We also study the distribution of θ_{K^+} ($\theta_{K_S^0}$), the angle between the K^+ (K_S^0) direction in the DK rest frame, and the DK direction in the laboratory frame. We expect the distribution of this angle to be symmetric around zero [10], but we observe an accumulation of combinatorial background close to $\cos\theta_K = -1$. Because of the jetlike nature of the reaction $e^+e^- \to c\bar{c}$, we interpret this background as due to combinations for which the K comes from the jet opposite to the D meson. We therefore apply a conservative cut requiring $\cos\theta_K > -0.8$.

The resulting D^0K^+ and $D^+K_S^0$ mass spectra are shown in Fig. 2. To improve the mass resolution, the nominal D mass and the reconstructed three-momentum are used to calculate the D energy for channels (1) and (2). The two mass spectra in Fig. 2 present similar features. The single bin peak at 2.4 GeV/c^2 results from decays of $D_{s1}(2536)^+$ to $D^{*0}K^+$ or $D^{*+}K_S^0$ in which the π^0 or γ from the D^* decay is missed. Since the $D_{s1}(2536)^+$ is believed to have $J^P = 1^+$, decay to DK is forbidden by angular momentum and parity conservation. We also observe a prominent narrow signal due to the $D_{s2}^*(2573)^+$, a broad structure centered at the mass of the $D_{s1}^*(2710)^+$, and a narrower structure at the position of the $D_{sJ}^*(2860)^+$.

We perform a simultaneous binned χ^2 fit to the two sideband-subtracted DK mass spectra shown in Figs. 3(a) and 3(c). The fit range extends from 2.42 GeV/c^2 to 3.2 GeV/c^2 [the lower bound is chosen to exclude the

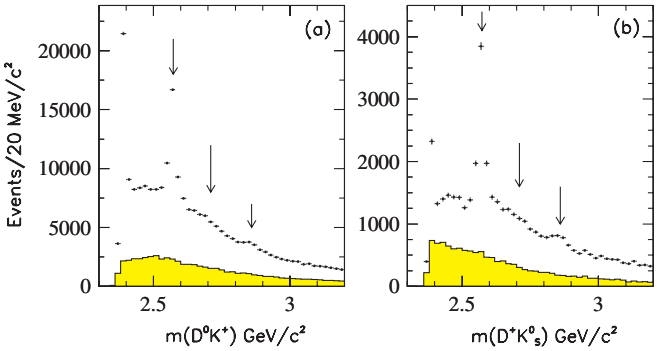

FIG. 2 (color online). DK invariant-mass distributions for (a) $D^0_{K^-\pi^+}K^+$ and (b) $D^+_{K^-\pi^+\pi^+}K_s^0$. Shaded histograms represent the D mass sideband regions. The arrows indicate the expected positions of the $D_{s2}^*(2573)^+$, $D_{s1}^*(2710)^+$, and $D_{sJ}^*(2860)^+$.

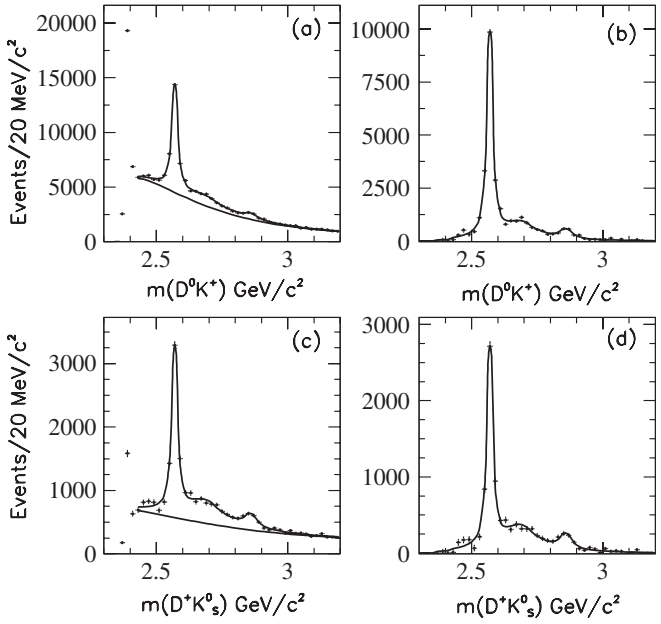

FIG. 3. Sideband-subtracted DK invariant-mass distributions for (a) $D^0_{K^-\pi^+}K^+$ and (c) $D^+_{K^-\pi^+\pi^+}K^0_S$; (b) and (d) show the fitted-background-subtracted mass spectra. The curves show the functions described in the text.

$D_{s1}(2536)^+$ reflection]. The background for each of the two DK mass distributions is described by a threshold function: $(m - m_{\rm th})^\alpha e^{-\beta m - \gamma m^2 - \delta m^3}$ where $m_{\rm th} = m_D + m_K$. In this fit, the $D^*_{s2}(2573)^+$, $D^*_{s1}(2710)^+$, and $D^*_{sJ}(2860)^+$ peaks are described with relativistic Breit-Wigner line shapes, where spin-2 is assumed for $D^*_{s2}(2573)^+$, spin-1 for $D^*_{s1}(2710)^+$, and spin-0 for $D^*_{sJ}(2860)^+$. The Breit-Wigner function includes Blatt-Weisskopf form factors [11]. Mass resolution estimates are obtained using simulated events. We obtain single-Gaussian σ's of 2.7 MeV/c^2 and 3.6 MeV/c^2 at DK masses of 2.71 and 2.86 GeV/c^2, respectively. Since the width values for the resonances present in the DK mass spectra are much larger than these, resolution effects are ignored.

The result of the fit is shown in Figs. 3(a) and 3(c), and the parameter values obtained are summarized in Table II (Fit A). Figures 3(b) and 3(d) show also the fitted-background-subtracted $D^0_{K^-\pi^+}K^+$, and $D^+_{K^-\pi^+\pi^+}K^0_S$ invariant-mass distributions. The fitted parameter values for the $D^*_{sJ}(2860)^+$ state are in agreement with our previous measurement [3], while the central value of the $D^*_{s1}(2710)^+$ mass is slightly higher than before.

V. STUDY OF THE D^*K SYSTEM

The $\Delta m = m(D\pi) - m(D)$ distributions for the five channels, (3)–(7), are shown in Fig. 4. Backgrounds are small for channels (5)–(7) but larger for channels (3)–(4). Table III gives the fitted parameter values of the Δm distributions together with purities and the definitions of signal and sideband regions. The values of σ reported in Table III are obtained from fits performed using a polynomial background and a single Gaussian.

We have also studied the distributions of the angle $\theta^*_{K^+}$ ($\theta^*_{K^0_S}$) between the K^+ (K^0_S) direction in the D^*K rest frame and the D^*K direction in the laboratory frame. We expect the distributions of this angle to be symmetric around zero for signal, but we observe an accumulation of combinatorial background close to $\cos\theta^*_K = -1$. As in the case of the DK system, we interpret this as being due to combinations

TABLE II. The χ^2/NDF and resonance parameter values obtained from the fits to the DK and D^*K mass spectra. Masses and widths are given in units of MeV/c^2 and MeV, respectively. Uncertainties are statistical only.

Fit	χ^2/NDF	$D^*_{s1}(2710)^+$	$D^*_{sJ}(2860)^+$	$D_{sJ}(3040)^+$
A (DK)	85/56	$m = 2710.0 \pm 3.3$ $\Gamma = 178 \pm 19$	$m = 2860.0 \pm 2.3$ $\Gamma = 53 \pm 6$	
B (D^*K)	51/33	$m = 2712 \pm 3$ $\Gamma = 103 \pm 8$	$m = 2865.2 \pm 3.5$ $\Gamma = 44 \pm 8.3$	$m = 3042 \pm 9$ $\Gamma = 214 \pm 34$
C ($DK + D^*K$)	147/91	$m = 2710 \pm 3$ $\Gamma = 152 \pm 7$	$m = 2860 \pm 2$ $\Gamma = 52 \pm 5$ $m = 2866 \pm 3$ $\Gamma = 43 \pm 6$	$m = 3045 \pm 8$ $\Gamma = 246 \pm 31$
D ($DK + D^*K$)	149/93	$m = 2710 \pm 2$ $\Gamma = 152 \pm 7$	$m = 2862 \pm 2$ $\Gamma = 48 \pm 3$	$m = 3044 \pm 8$ $\Gamma = 239 \pm 35$
E (D^*K)	65/38	$m = 2716.7 \pm 2.5$ $\Gamma = 108 \pm 5$		
F (D^*K)	39/34			$m = 3047 \pm 12$ $\Gamma = 216 \pm 46$

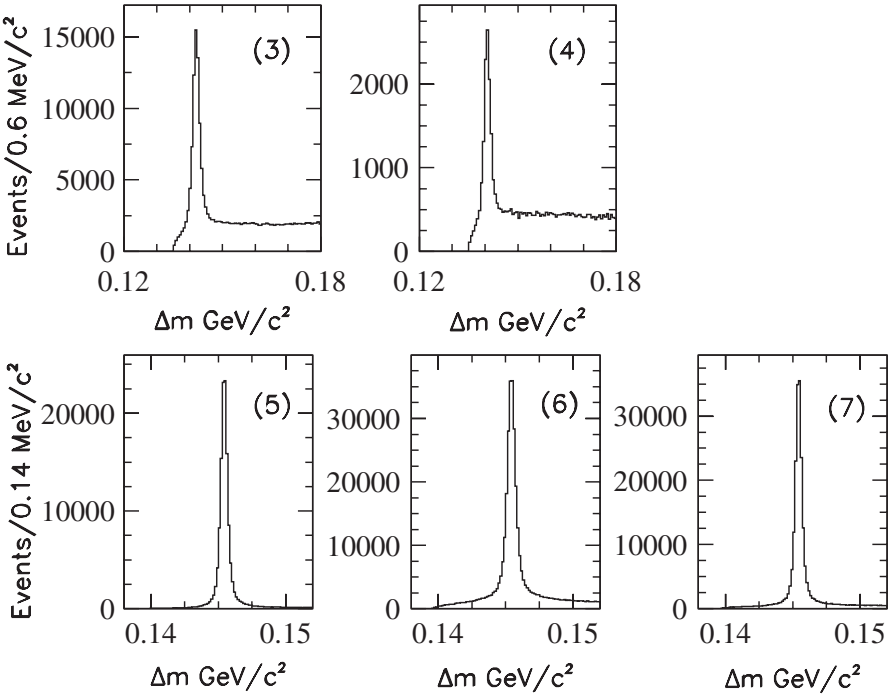

FIG. 4. The Δm distributions for channels (3)–(7) after applying the corresponding D-candidate mass selection criteria.

for which the K comes from the jet opposite to that yielding the D^* meson. We therefore apply the conservative selection criterion $\cos\theta_K^* > -0.8$.

Figure 5 shows the reconstructed D^*K mass spectra for channels (3)–(7) of Table I. The shaded distributions represent the background estimates from the Δm sideband regions. Each distribution shows a narrow spike at threshold due to the $D_{s1}(2536)^+$ meson. We also observe structures around 2.71 and 2.86 GeV$/c^2$.

We have compared these mass spectra with those from generic $e^+e^- \to \bar{c}c$ Monte Carlo events. These events were generated using a detailed detector simulation and subjected to the same reconstruction and event-selection procedure as used for the data. We find that the simulation underestimates the $D_{s1}(2536)^+$ and $D_{s2}^*(2573)^+$ signals relative to the background. No such discrepancy is found in the study of nonstrange final states; therefore, we attribute this effect to poor knowledge of the strange-charmed meson cross sections [12]. We apply weights to the $D_{s1}(2536)^+$ and $D_{s2}^*(2573)^+$ production in the Monte Carlo events in order to obtain better agreement with the data.

Diagram (3) of Fig. 5 shows the presence of a peaking background in channel (3) around 2.7 GeV$/c^2$. Using the Monte Carlo data we identify this reflection, which is present in the signal and the sideband regions, as being due to the $D_{s2}^*(2573)^+$. Combinations of DK originating from this narrow peak associate with a random π^0 to produce a relatively narrow structure in the 2.7 GeV$/c^2$ region. Our Monte Carlo study verifies that this reflection is almost completely removed by performing the Δm sideband subtraction.

The total D^*K mass spectrum, Δm-sideband-subtracted and summed over channels (3)–(7), is shown in Fig. 6 and compared with that obtained from Monte Carlo simulations. The D^*K mass spectrum, above the $D_{s1}(2536)^+$ signal, shows the presence of structures around 2.71, 2.86, and 3.04 GeV$/c^2$. Corresponding resonance contri-

TABLE III. Fitted parameters of the Δm distributions together with purities and definitions of the regions used for signal and background.

Channel	Mass MeV$/c^2$	σ MeV$/c^2$	Purity (%)	Signal region	Sideband region
(3) $\Delta m(D^0_{K^-\pi^+}\pi^0)$	142.02	1.08	83.3	$\pm 2.5\sigma$	10σ–15σ
(4) $\Delta m(D^+_{K^-\pi^+\pi^+}\pi^0)$	140.63	0.893	76.6	$\pm 2.5\sigma$	10σ–15σ
(5) $\Delta m(D^0_{K^-\pi^+}\pi^+)$	145.43	0.288	94.9	$\pm 5\sigma$	12σ–22σ
(6) $\Delta m(D^0_{K^-\pi^+\pi^0}\pi^+)$	145.43	0.351	87.1	$\pm 3\sigma$	10σ–16σ
(7) $\Delta m(D^0_{K^-\pi^+\pi^+\pi^-}\pi^+)$	145.43	0.266	90.5	$\pm 5\sigma$	12σ–22σ

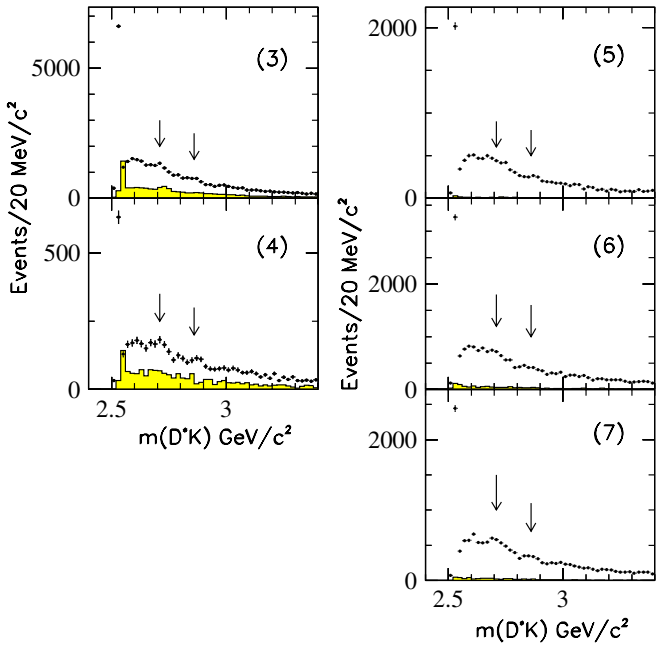

FIG. 5 (color online). The $m(D^*K)$ distributions for channels (3)–(7); the shaded histograms show the mass spectra from the D^* Δm sideband regions. The arrows indicate the expected positions of the $D^*_{s1}(2710)^+$ and $D^*_{sJ}(2860)^+$.

butions are not included in the Monte Carlo simulations. Since such enhancements are not evident in the Monte Carlo D^*K mass spectrum, we conclude that these structures are not produced by reflections from known resonances. Monte Carlo simulations also show that these enhancements are not due to reflections from the D_{sJ} resonances observed in the DK mass spectrum.

A structure close to 2.57 GeV/c^2 is seen in the Monte Carlo mass spectrum and is due to the decay $D^*_{s2}(2573)^+ \to D^*K$, included in the simulations. However, the data do not show evidence for such a decay.

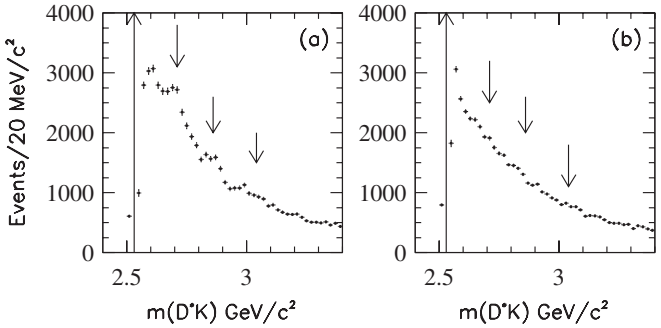

FIG. 6. The sideband-subtracted $m(D^*K)$ distributions summed over channels (3)–(7). Panel (a) is for data, and (b) for Monte Carlo. The arrow near threshold indicates the position of the peak due to the $D_{s1}(2536)^+$, which is off scale. The other arrows indicate the expected positions of the $D^*_{s1}(2710)^+$, $D^*_{sJ}(2860)^+$, and $D_{sJ}(3040)^+$.

VI. FITS TO THE D^*K MASS SPECTRUM

We perform a binned minimum χ^2 fit to the combined D^*K mass spectrum. The fit is performed in the region (2.58–3.48) GeV/c^2. The background is parametrized as $e^{-\beta m-\gamma m^2-\delta m^3}$, which provides a good description of the Monte Carlo in the same mass range. The D^+_{sJ} peaks are described with relativistic Breit-Wigner line shapes. Here and in the following fits, we assume $J^P = 1^-$ and $J^P = 3^-$, respectively, for $D^*_{s1}(2710)^+$ and $D^*_{sJ}(2860)^+$ decays to DK. For the D^*K system, we use an angular momentum $L = 1$, $L = 3$, and $L = 0$ for $D^*_{s1}(2710)^+$, $D^*_{sJ}(2860)^+$, and $D_{sJ}(3040)^+$, respectively. Average mass resolutions are 2.5 MeV/c^2 and 3.5 MeV/c^2 at D^*K masses of 2.71 and 2.86 GeV/c^2, respectively. Since the width values for the resonances present in the D^*K mass spectra are much larger than these, resolution effects are ignored.

We observe the presence, above the $D^*_{s1}(2710)^+$ and $D^*_{sJ}(2860)^+$, of a new broad structure peaking at 3.04 GeV/c^2. The resonance parameters resulting from the fit are given in Table II (Fit B) and the corresponding fitted curves are shown in Fig. 7. Modifying the background to include an extra term in the exponential does not improve the fit significantly. We find that the width of the $D^*_{s1}(2710)^+$ differs somewhat between the DK and D^*K fits, while the parameter values for the structure at 2.86 GeV/c^2 in the D^*K mass spectrum are consistent with those of the $D^*_{sJ}(2860)^+$ obtained from the DK mass spectrum.

We next repeat the fits, removing the resonances one by one from the probability density function. We compute the statistical significance of each structure as $\sqrt{\Delta\chi^2}$, where $\Delta\chi^2$ is the difference in the fit χ^2 with and without the resonance included, taking into account the variation in the number of parameters (ΔNDF = 3). We obtain statistical significances of 12.4, 6.4, and 6.0 standard deviations for the $D^*_{s1}(2710)^+$, $D^*_{sJ}(2860)^+$, and $D_{sJ}(3040)^+$, respectively.

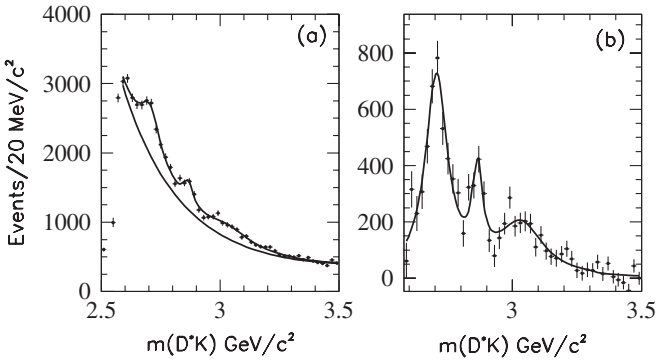

FIG. 7. (a) Fit to the D^*K invariant-mass spectrum. (b) Residuals after subtraction of the fitted background. The curves are described in the text.

We then perform simultaneous fits to the two DK mass spectra and to the total D^*K mass spectrum to better constrain the $D^*_{s1}(2710)^+$ parameters. We first test the possibility that the structure around 2.86 GeV/c^2 in the D^*K mass spectrum is different from the $D^*_{sJ}(2860)^+$ state observed in the DK mass spectrum by adding to the fit two new parameters. The results from the fit are summarized in Table II (Fit C). We find the parameters of the $D^*_{sJ}(2860)^+$ in the DK mass spectrum consistent with those measured in the D^*K mass spectrum.

Assuming therefore that we are observing the same state, we constrain the $D^*_{sJ}(2860)^+$ parameters to be the same in both the DK and D^*K mass spectra (Fit D). Taking this as our reference fit, we obtain the following parameters for the three states:

$$m(D^*_{s1}(2710)^+) = 2710 \pm 2_{\rm stat}(^{+12}_{-7})_{\rm syst}\ {\rm MeV}/c^2,$$
$$\Gamma = 149 \pm 7_{\rm stat}(^{+39}_{-52})_{\rm syst}\ {\rm MeV}, \quad (1)$$

$$m(D^*_{sJ}(2860)^+) = 2862 \pm 2_{\rm stat}(^{+5}_{-2})_{\rm syst}\ {\rm MeV}/c^2,$$
$$\Gamma = 48 \pm 3_{\rm stat} \pm 6_{\rm syst}\ {\rm MeV}, \quad (2)$$

$$m(D_{sJ}(3040)) = 3044 \pm 8_{\rm stat}(^{+30}_{-5})_{\rm syst}\ {\rm MeV}/c^2,$$
$$\Gamma = 239 \pm 35_{\rm stat}(^{+46}_{-42})_{\rm syst}\ {\rm MeV}. \quad (3)$$

Here systematic uncertainties take into account the range of values obtained in different fits, including fits to the spectra obtained after modifying the p^* selection criterion, modifying the Δm criteria, and removing the $\cos\theta_K$ requirement. They also account for uncertainties in the spin assignment.

VII. ANGULAR ANALYSIS

Since we observe both $D^*_{s1}(2710)^+$ and $D^*_{sJ}(2860)^+$ decays to both DK and D^*K, we assume they have natural parity $J^P = 1^-, 2^+, 3^-, \ldots$ ($J^P = 0^+$ is ruled out because of the D^*K decay). We further test this hypothesis using angular analysis. We compute the helicity angle θ_h as the angle formed by the π from the D^* decay with respect to the kaon, in the D^* rest frame. The angular distribution for natural parity is expected to be [13]

$$\frac{dN}{d\cos\theta_h} \cong 1 - \cos^2\theta_h, \quad (4)$$

since, for the parity and angular momentum conserving decay of such a parent state, the coupling in the parent rest frame to the helicity-0 D^* state involves a vanishing Clebsch-Gordan coefficient. Figure 8 shows the D^*K mass spectrum separated for $|\cos\theta_h| < 0.4$ [(a), (b)] and $|\cos\theta_h| > 0.4$ [(c), (d)]. We clearly observe an enhanced signal-to-background rate for the $D^*_{s1}(2710)^+$ in the $|\cos\theta_h| < 0.4$ region. This does not hold for the $D_{sJ}(3040)^+$. The nonobservation of $D_{sJ}(3040)^+ \to DK$ also suggests unnatural parity for this state.

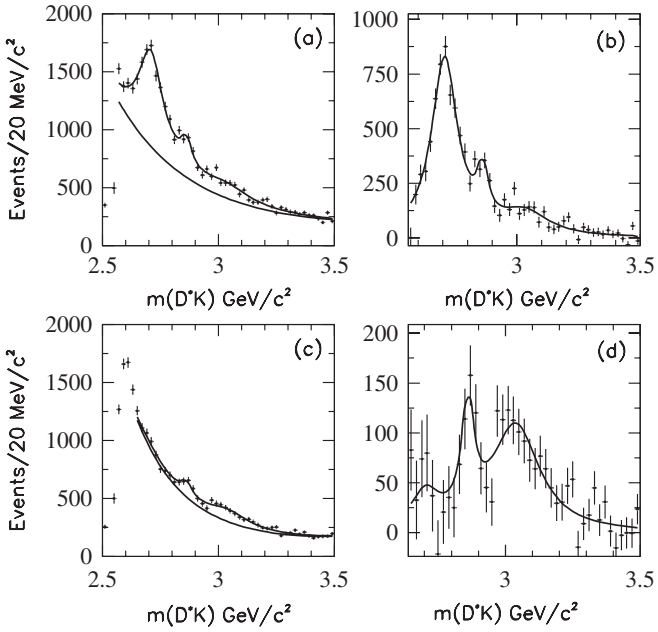

FIG. 8. Fits to the D^*K invariant-mass spectra for (a) $|\cos\theta_h| < 0.4$ and (c) $|\cos\theta_h| > 0.4$. (b) and (d) show the data after the fitted background is subtracted.

The mass spectra separated according to the value of $|\cos\theta_h|$ allow a better determination of the $D^*_{s1}(2710)^+$ and $D_{sJ}(3040)^+$ parameters. When fitting the $|\cos\theta_h| < 0.4$ data (Fit E) we fix the $D^*_{sJ}(2860)^+$ and $D_{sJ}(3040)^+$ shape parameters to those resulting from the simultaneous fit of the DK and D^*K mass spectra (Fit D). In fitting the $|\cos\theta_h| > 0.4$ data (Fit F) we fix the parameters of $D^*_{s1}(2710)^+$ and $D^*_{sJ}(2860)^+$ to those from Fit D. The resulting $D^*_{s1}(2710)^+$ and $D_{sJ}(3040)^+$ parameters are given in Table II, and the fit results are shown by the curves in Fig. 8.

We have studied the $\cos\theta_h$ distributions for the $D^*_{s1}(2710)^+$ and $D^*_{sJ}(2860)^+$ by producing D^*K mass spectra in six intervals of $\cos\theta_h$. The mass spectrum in each interval was fitted with fixed resonance parameters. However, these values have all been varied within their statistical and systematic errors. The efficiencies as a function of $\cos\theta_h$ in the two mass regions are obtained from Monte Carlo simulation of the five channels involved in the analysis. We find that the efficiency is almost uniform as a function of $\cos\theta_h$ with a small slope which we parametrize by a linear function.

The efficiency-corrected $D^*_{s1}(2710)^+$ and $D^*_{sJ}(2860)^+$ yields are plotted in Fig. 9, together with the normalized expectations for natural parity. The curves have χ^2/NDF of 18.7/5 and 6.3/5, respectively. The large χ^2 obtained for the $D^*_{s1}(2710)^+$ is related to the large uncertainties in the background parametrization. Other spin hypotheses have been tested but they give much larger χ^2 values. We conclude that both states are consistent with having natural parity. We do not perform a similar analysis for

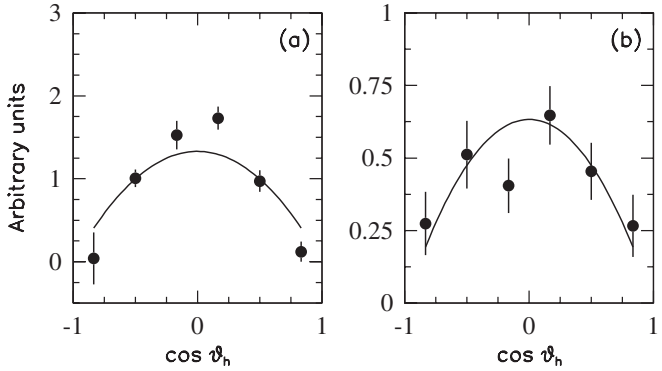

FIG. 9. Distributions in $\cos\theta_h$ for (a) $D_{s1}^*(2710)^+$ and (b) $D_{sJ}^*(2860)^+$.

$D_{sJ}(3040)^+$ because of the large uncertainties arising from fitting a very broad resonance with limited statistics.

VIII. BRANCHING FRACTIONS

From Table I it can be seen that it is possible to obtain ratios of branching fractions with reduced systematic uncertainties, for $D_{s1}^*(2710)^+$ and $D_{sJ}^*(2860)^+$ by using channels (3), (1) and (4), (2), respectively.

These ratios are computed as

$$r_i = \frac{N(D_{sJ}^* \to D^*K)}{N(D_{sJ}^* \to DK)} \frac{\epsilon(D_{sJ}^* \to DK)}{\epsilon(D_{sJ}^* \to D^*K)}, \tag{5}$$

where the $N(D_{sJ}^*)$ are the signal yields and the $\epsilon(D_{sJ}^*)$ are the corresponding efficiencies, and $i = 1, 4$. We note that the only difference between numerator and denominator final states is the presence of an extra π^0 from the D^* decay.

Assuming a constant total width, the yields are obtained by fitting the DK and D^*K mass spectra using the same $D_{s1}^*(2710)^+$ and $D_{sJ}^*(2860)^+$ parameters, and are summarized in Table IV. Efficiencies are evaluated using Monte Carlo simulations, and only the ratio of efficiencies

$$\epsilon_r = \frac{\epsilon(D_{sJ}^* \to D^*K)}{\epsilon(D_{sJ}^* \to DK)} \tag{6}$$

is involved in the measurement. This ratio is consistent with being uniform as a function of $DK(D^*K)$ mass, and its values are reported in Table IV.

Systematic uncertainties are summarized in Table V. The D_{sJ}^* parameters have been varied within their statistical and systematic errors, the p^* cut has been changed to 3.1 and 3.5 GeV/c, and the $\cos\theta_K$ cuts have been increased to -0.6. The systematic error arising from Monte Carlo statistics appears as the error on the ratio between the efficiencies. The error on the D^* branching fractions is obtained from Ref. [14]. The shape of the background has been modified by adding an extra term in the exponential; its contribution to the total error is found to be negligible. Finally, the D^* Δm signal region has been reduced to $\pm 2\sigma$.

We obtain the following ratios of branching fractions:

$$r_1 = \frac{\mathcal{B}(D_{s1}^*(2710)^+ \to D^{*0}K^+)}{\mathcal{B}(D_{s1}^*(2710)^+ \to D^0K^+)} = 0.88 \pm 0.14_{\text{stat}} \pm 0.14_{\text{syst}}, \tag{7}$$

$$r_2 = \frac{\mathcal{B}(D_{sJ}^*(2860)^+ \to D^{*0}K^+)}{\mathcal{B}(D_{sJ}^*(2860)^+ \to D^0K^+)} = 1.04 \pm 0.17_{\text{stat}} \pm 0.20_{\text{syst}}, \tag{8}$$

where $D^{*0} \to D^0\pi^0$, and

$$r_3 = \frac{\mathcal{B}(D_{s1}^*(2710)^+ \to D^{*+}K_S^0)}{\mathcal{B}(D_{s1}^*(2710)^+ \to D^+K_S^0)} = 1.14 \pm 0.39_{\text{stat}} \pm 0.23_{\text{syst}}, \tag{9}$$

$$r_4 = \frac{\mathcal{B}(D_{sJ}^*(2860)^+ \to D^{*+}K_S^0)}{\mathcal{B}(D_{sJ}^*(2860)^+ \to D^+K_S^0)} = 1.38 \pm 0.35_{\text{stat}} \pm 0.49_{\text{syst}}, \tag{10}$$

where $D^{*+} \to D^+\pi^0$.

TABLE IV. Information related to the evaluation of the ratio of branching fractions for the D_{sJ}^* resonances.

Decay	N	ϵ_r	D^* B.F. (%)	r_i
$D_{s1}^*(2710)^+ \to D^0K^+$	6469 ± 425			
$D_{s1}^*(2710)^+ \to D^{*0}K^+$	1247 ± 173	0.353 ± 0.005	61.9 ± 2.9	0.88 ± 0.14
$D_{sJ}^*(2860)^+ \to D^0K^+$	1826 ± 158			
$D_{sJ}^*(2860)^+ \to D^{*0}K^+$	415 ± 55			1.04 ± 0.17
$D_{s1}^*(2710)^+ \to D^+K_S^0$	2442 ± 179			
$D_{s1}^*(2710)^+ \to D^{*+}K_S^0$	258 ± 75	0.301 ± 0.009	30.7 ± 0.5	1.14 ± 0.39
$D_{sJ}^*(2860)^+ \to D^+K_S^0$	781 ± 83			
$D_{sJ}^*(2860)^+ \to D^{*+}K_S^0$	100 ± 23			1.38 ± 0.35

TABLE V. Systematic uncertainties in the evaluation of the ratio of branching fractions.

Ratio	D_{sJ} parameters	MC statistics	D^* B.F.	p^* cut	$\cos\theta_K$ cut	Δm cut	Total
r_1	0.030	0.013	0.042	0.018	0.120	0.044	0.14
r_2	0.050	0.015	0.050	0.066	0.175	0.004	0.20
r_3	0.077	0.033	0.018	0.042	0.128	0.160	0.23
r_4	0.106	0.040	0.022	0.009	0.328	0.345	0.49

Averaging r_1, r_3 and r_2, r_4, we obtain

$$\frac{\mathcal{B}(D_{s1}^*(2710)^+ \to D^*K)}{\mathcal{B}(D_{s1}^*(2710)^+ \to DK)} = 0.91 \pm 0.13_{\text{stat}} \pm 0.12_{\text{syst}}, \tag{11}$$

$$\frac{\mathcal{B}(D_{sJ}^*(2860)^+ \to D^*K)}{\mathcal{B}(D_{sJ}^*(2860)^+ \to DK)} = 1.10 \pm 0.15_{\text{stat}} \pm 0.19_{\text{syst}}. \tag{12}$$

We also make a test of isospin conservation. We use the yields obtained from the fit to the appropriate mass spectra and correct for efficiency and branching fractions. We obtain, within the errors, similar rates for resonance decays to D^0K^+ and $D^+K_S^0$ as well as for decays to $D^{*0}K^+$ and $D^{*+}K_S^0$, as expected from isospin conservation.

We now compare these results with theoretical expectations. In the work of Ref. [15], for $J^P = 1^-$, two different quark model assignments are proposed for the $D_{s1}^*(2710)^+$: the $l = 2$ ground state, 1^3D_1, and the $l = 0$ first radial excitation, 2^3S_1. In the first case the ratio $\mathcal{B}(D_{s1}^*(2710) \to D^*K)/\mathcal{B}(D_{s1}^*(2710) \to DK)$ is expected to be 0.043 ± 0.002, in the second case 0.91 ± 0.04. In this framework the $D_{s1}^*(2710)^+$ can be identified as the first radial excitation of the $D_s^*(2112)$. The same assignment is derived from Ref. [6], where a mass of 2711 MeV/c^2 is predicted for the state 2^3S_1. However, in this case the expected ratio is 3.55, in significant disagreement with the measured value.

In Ref. [16], in the framework of chiral doublers, $J^P = 1^-$ states are expected at masses of 2632 and 2720 MeV/c^2.

The observation of $D_{sJ}^*(2860)^+ \to D^*K$ rules out the $J^P = 0^+$ assignment suggested by Refs. [5,6]. In Ref. [7] the $J^P = 3^-$ assignment is proposed; however, the predicted $\mathcal{B}(D_{sJ}^*(2860) \to D^*K)/\mathcal{B}(D_{sJ}^*(2860) \to DK)$ is 0.39, which differs from our measurement at the level of 3 standard deviations. A better agreement is obtained if we compare with the calculations from Ref. [17], which expects a ratio of 0.6.

As to the possible interpretation of the $D_{sJ}(3040)^+$ state, we note that Ref. [18] predicts two $J^P = 1^+$ radial excitations at 3082 and 3094 MeV/c^2.

IX. CONCLUSIONS

In summary, in 470 fb^{-1} of data collected by the *BABAR* experiment, we observe the decays of the $D_{s1}^*(2710)^+$ and $D_{sJ}^*(2860)^+$ to D^*K and measure their branching fractions relative to DK. A new, broad D_{sJ}^+ state is observed in the D^*K mass spectrum at a mass near 3040 GeV/c^2. Possible spin-parity assignments for these states are discussed.

ACKNOWLEDGMENTS

We are grateful for the extraordinary contributions of our PEP-II colleagues in achieving the excellent luminosity and machine conditions that have made this work possible. The success of this project also relies critically on the expertise and dedication of the computing organizations that support *BABAR*. The collaborating institutions wish to thank SLAC for its support and the kind hospitality extended to them. This work is supported by the U.S. Department of Energy and National Science Foundation, the Natural Sciences and Engineering Research Council (Canada), the Commissariat à l'Energie Atomique and Institut National de Physique Nucléaire et de Physique des Particules (France), the Bundesministerium für Bildung und Forschung and Deutsche Forschungsgemeinschaft (Germany), the Istituto Nazionale di Fisica Nucleare (Italy), the Foundation for Fundamental Research on Matter (The Netherlands), the Research Council of Norway, the Ministry of Education and Science of the Russian Federation, Ministerio de Educación y Ciencia (Spain), and the Science and Technology Facilities Council (United Kingdom). Individuals have received support from the Marie-Curie IEF program (European Union) and the A. P. Sloan Foundation.

[1] B. Aubert *et al.* (*BABAR* Collaboration), Phys. Rev. Lett. **90**, 242001 (2003); D. Besson *et al.* (CLEO Collaboration), Phys. Rev. D **68**, 032002 (2003); K. Abe *et al.* (Belle Collaboration), Phys. Rev. Lett. **92**, 171802

(2004); B. Aubert *et al.* (*BABAR* Collaboration), Phys. Rev. D **69**, 031101 (2004).
[2] S. Godfrey and N. Isgur, Phys. Rev. D **32**, 189 (1985); S. Godfrey and R. Kokoski, Phys. Rev. D **43**, 1679 (1991); N. Isgur and M. B. Wise, Phys. Rev. Lett. **66**, 1130 (1991); M. Di Pierro and E. Eichten, Phys. Rev. D **64**, 114004 (2001); T. Matsuki, T. Morii, and K. Sudoh, Prog. Theor. Phys. **117**, 1077 (2007).
[3] B. Aubert *et al.* (*BABAR* Collaboration), Phys. Rev. Lett. **97**, 222001 (2006).
[4] J. Brodzicka *et al.* (Belle Collaboration), Phys. Rev. Lett. **100**, 092001 (2008).
[5] E. van Beveren and George Rupp, Phys. Rev. Lett. **97**, 202001 (2006).
[6] F. E. Close, C. E. Thomas, O. Lakhina, and E. S. Swanson, Phys. Lett. B **647**, 159 (2007).
[7] P. Colangelo, F. De Fazio, and S. Nicotri, Phys. Lett. B **642**, 48 (2006).
[8] B. Aubert *et al.* (*BABAR* Collaboration), Nucl. Instrum. Methods Phys. Res., Sect. A **479**, 1 (2002).
[9] The use of charge-conjugate reactions is implied throughout.
[10] T. Bergfeld *et al.* (CLEO Collaboration), Phys. Lett. B **340**, 194 (1994).
[11] J. M. Blatt and V. F. Weisskopf, *Theoretical Nuclear Physics* (John Wiley & Sons, New York, 1952).
[12] G. D. Lafferty, P. I. Reeves, and M. R. Whalley, J. Phys. G **21**, A1 (1995).
[13] P. Avery *et al.* (CLEO Collaboration), Phys. Lett. B **331**, 236 (1994); **342**, 453(E) (1995).
[14] C. Amsler *et al.* (Particle Data Group), Phys. Lett. B **667**, 1 (2008).
[15] P. Colangelo, F. De Fazio, S. Nicotri, and M. Rizzi, Phys. Rev. D **77**, 014012 (2008).
[16] M. A. Nowak, M. Rho, and I. Zahed, Acta Phys. Pol. B **35**, 2377 (2004).
[17] B. Zhang, X. Liu, W. Z. Deng, and S. L. Zhu, Eur. Phys. J. C **50**, 617 (2007).
[18] T. Matsuki, T. Morii, and K. Sudoh, Eur. Phys. J. A **31**, 701 (2007).